Spectroscopy and electronic structure of jet-cooled GaAs

George W. Lemire, Gregory A. Bishea, Scott A. Heidecke, and Michael D. Morse
Department of Chemistry, University of Utah, Salt Lake City, Utah 84112

(Received 1 September 1989; accepted 29 September 1989)

An optical spectrum, obtained by resonant two-photon ionization spectroscopy, is reported for jet-cooled diatomic gallium arsenide. The ground state is identified as $X\,^3\Sigma^-$, deriving from a $\sigma^2\pi^2$ molecular configuration, and is characterized by $\omega_e'' = 215\ \text{cm}^{-1}$, $\omega_e''x_e'' = 3\ \text{cm}^{-1}$, and $r_0'' = 2.53 \pm 0.02$ Å. The upper state of the observed band system is $^3\Pi_r$, correlating to the Ga $4s^24p$, $^2P^0$ + As $4s^24p^3$, $^2D^0$ excited separated atom limit. A strong predissociation sets in above $v' = 0$ for the $\Omega' = 2,1$ and 0^- components of the $^3\Pi_r$ excited state, and it is proposed that this is induced by spin–orbit interaction with the $\sigma\sigma^*\pi^2$, $^5\Sigma^-$ state which correlates to ground state atomic fragments. Constants for the upper $^3\Pi_{0+}$ state are $\omega_e' = 152.13 \pm 0.70\ \text{cm}^{-1}$, $\omega_e'x_e' = 2.89 \pm 0.08\ \text{cm}^{-1}$, and $r_e' = 2.662 \pm 0.027$ Å for the $^{69}Ga^{75}As$ isotopic modification. The ionization potential of GaAs has been bracketed as IP(GaAs) $= 7.17 \pm 0.75$ eV, and a re-evaluation of the third-law measurement of the bond strength provides $D_0(\text{GaAs}) = 2.06 \pm 0.05$ eV. Comparisons to group IV and other group III-V diatomics, and to the bulk solid materials are also presented.

I. INTRODUCTION

Gallium arsenide has been a subject of intense interest in the electronics industry for some 20 to 30 years, owing to its favorable properties as a semiconducting material.[1,2] Physically and electronically, GaAs is similar to the homogeneous semiconductors silicon and germanium. As a compound semiconductor, however, GaAs possesses a significant degree of charge polarization. The possibility of charge transfer from gallium to arsenic adds an ionic component to the chemical bonding, which causes the band gap in GaAs (1.42 eV[1]) to be larger than in either silicon (1.08 eV[1]) or germanium (0.67 eV[3]). This larger band gap increases the electrical resistivity of high-purity GaAs as compared to Si or Ge, thereby increasing the range of resistivity which is available through doping.[1] The large band gap of GaAs also allows semiconducting behavior to be maintained to higher temperatures than in the homogeneous semiconductors.[1] Furthermore, mixed III–V semiconductors such as $Ga_{1-x}Al_xAs$ allow one to continuously tune the band gap and other electronic properties to suit the desired application. Finally, the much lighter effective mass of an electron in the conduction band of GaAs ($0.063\ m_0$)[1] as compared to Si ($0.3\ m_0$)[1] implies that it should be possible to construct much faster electronic devices using gallium arsenide instead of silicon. Together, all of these advantages make gallium arsenide extremely exciting as an electronic material, and account for the tremendous research effort directed toward the eventual commercialization of gallium arsenide technology.

With this level of interest in bulk GaAs, it is surprising that almost no experimental data are currently available on diatomic GaAs. In this paper we report the first spectroscopic study of gaseous GaAs, in which we present a detailed investigation of the $^3\Pi \leftarrow X\,^3\Sigma^-$ electronic band system, located between 432 and 409 nm. This band system, which we have obtained in a resonant two-photon ionization study of jet-cooled GaAs, may be useful in probing the reaction mechanism of organometallic vapor-phase epitaxial growth of GaAs films on suitable substrates.[1,2,4–6] This is a promising avenue for the production of electronic devices employing gallium arsenide circuitry, in which organometallic precursors such as trimethylgallium [$Ga(CH_3)_3$] and arsine (AsH_3) are pyrolyzed, resulting in epitaxial deposition of GaAs. Little is currently known about the detailed kinetics of such processes,[5] and it is possible that gaseous GaAs may play a role in the reaction mechanism. The spectrum which we report in this paper provides a fingerprint, which through laser-induced fluorescence or resonant two-photon ionization spectroscopy may help to sort out the role of gaseous GaAs in the mechanism of pyrolytic epitaxial deposition of GaAs films.

In addition to the potential technological benefits of spectroscopic work on diatomic GaAs, it is of interest to examine the electronic structure of this molecule in the context of periodic trends. Diatomic GaAs is isoelectronic with Ge_2 and is isovalent with all of the group IV dimers and mixed group III–V diatomics. Spectroscopic data are already available for several of these species, including C_2,[7] Si_2,[8,9] Sn_2,[10] Pb_2,[11] SiC,[12] and BN.[13–15] It will be of interest to compare the electronic structure and chemical bonding of these species to that of GaAs, particularly since GaAs is the only heavy III–V diatomic for which spectroscopic data are now available. This comparison is provided in Sec. IV below.

The potential technological importance of GaAs as a semiconducting material has resulted in numerous theoretical studies of its bulk properties.[16–18] A logical extension of this theoretical work would be an investigation of gallium arsenide clusters as a function of size. Although this has not yet been done on a molecular level for any system in absolute detail, it remains a major goal in cluster science. Experimental approaches probing the size dependent properties of GaAs clusters were first reported from Smalley's research group.[19,20] This work demonstrated that large clusters formed by laser vaporization of GaAs exhibit a binomial distribution indicative of a statistical distribution of cluster compositions ranging from Ga_n to As_n, although smaller

 0021-9606/90/010121-12$03.00

clusters showed a narrower distribution favoring equal numbers of gallium and arsenic atoms.[19] In subsequent work the electron affinity of gallium arsenide clusters was bracketed as a function of cluster size, and photodissociation of $Ga_xAs_y^-$ anions was also reported.[20] More recently, $Ga_xAs_y^-$ anions have been reacted with HCl in an FT-ICR mass spectrometer,[21] demonstrating that etching proceeds by the reaction

$$Ga_xAs_y^- + HCl \rightarrow Ga_{x-1}As_yH^- + GaCl.$$

Moreover, these studies have established that $GaAs_4^-$, $Ga_2As_3^-$, $GaAs_4H^-$, $Ga_4As_2^-$ and $Ga_2As_4^-$ exhibit dual populations that can be kinetically differentiated, thereby demonstrating that these species exist in at least two isomeric forms.[21] This possibility had been anticipated by Balasubramanian, who has enumerated the structural isomers of Ga_xAs_y, and has suggested that several isomers of Ga_3As_3 should be possible.[22] Balasubramanian has also performed CASSCF-CI calculations on GaAs, $GaAs^+$, and $GaAs_2$,[23,24] and has predicted ground states of $^3\Sigma^-$ for GaAs, $^4\Sigma^-$ for $GaAs^+$, and $^2B_2$ for $GaAs_2$. A very recent MRD-CI study of GaAs and $GaAs^+$ also predicts a $^3\Sigma^-$ ground state for GaAs and $^4\Sigma^-$ for $GaAs^+$, along with detailed information about many excited states.[25] An electron spin resonance (ESR) investigation of $GaAs^+$ by Knight *et al.* has confirmed $^4\Sigma^-$ as the ground state of $GaAs^+$.[26] In the present work we confirm $^3\Sigma^-$ as the ground state of GaAs.

Before reporting our results, a description of the experimental method is presented in Sec. II. Section III presents our results, while the implications of our findings are given in Sec. IV. Section V then completes the paper with a summary of our major conclusions.

II. EXPERIMENTAL

The laser vaporization-supersonic expansion apparatus used in the present investigation is essentially the same as that employed in our previous studies of Al_3,[27] C_3,[28] Pt_2,[29] and NiCu.[30] The only real differences compared to previous experiments were minor modifications in the cluster source, as required by the GaAs substrate, and the use of suitable wavelengths for the resonant two-photon ionization (R2PI) process.

Although GaAs powder is available, the standard form used in the electronics industry consists of wafers 2 or 3 in. in diameter, 0.016–0.025 in. thick. The material is crystalline and quite brittle, and cannot be readily fabricated into the 0.125 in. diameter rods which our instrument was originally designed to accept. Therefore we obtained gallium arsenide wafers from Standard Oil Research and Development (Ohio), Morgan Semiconductor, and wafer fragments from Cominco Electronic Materials. The constraints associated with working with thin, brittle wafers required that the laser vaporization beam source be modified; accordingly we constructed a rotating-disk laser-vaporization source similar to that originally developed by O'Brien *et al.* for work with gallium arsenide.[19] In our version of this source the GaAs wafer is held directly against a flat stainless steel block by a spring-loaded flexible coupling. The vaporization laser is focused through a small channel in the stainless steel block onto the GaAs wafer, which is rotated at a rate of 0.3 rpm. The wafer is also translated back and forth at a rate of 0.04 rpm using a rotating eccentric cam, thereby allowing an annular region of the GaAs surface to be exposed to the vaporization laser. A channel carrying high-pressure helium lies just under the surface of the stainless steel block, intersecting the vaporization laser channel just below the point of vaporization. This channel then extends further, beyond the point of vaporization, providing a region in which clusters (or at least diatomic GaAs molecules) may form. Finally, expansion into vacuum occurs 2.5 cm beyond the point of vaporization, resulting in supersonic cooling of GaAs and the other species which may be present.

In contrast to the work of O'Brien *et al.*[19] and of Liu *et al.*,[20] our interest was directed toward the spectroscopy of diatomic GaAs, and production of larger clusters was undesirable. Although one might think that the resonant two-photon ionization (R2PI) scheme, coupled with mass spectrometric detection, would allow one to cleanly separate signals originating from larger clusters from those of the species of interest, this is not always the case. In unfavorable cases photoionization and photofragmentation of larger clusters can lead to a false signal in a lighter mass channel. If this false signal dominates over the true R2PI signal of the species of interest, it may totally obscure a spectroscopic transition, leading to a null result. For this reason we purposely avoided the use of a long clustering/thermalization region in our experiments, as was employed by both O'Brien *et al.*[19] and Liu *et al.*[20] in their studies of Ga_xAs_y clusters containing up to 30 atoms.

As in previous studies from our group,[27–30] vaporization of GaAs was achieved by focusing the second harmonic radiation of a Nd:YAG laser (Quantel, model 580-10, 532 nm, 20–25 mJ/pulse, focused to a spot size of about 1 mm) onto a GaAs target. The timing of the vaporization pulse is set to coincide with the peak density of helium carrier gas, which is pulsed over the surface of the target using a double-solenoid pulsed valve.[31] The helium carrier gas is maintained at a stagnation pressure of 120 psi, and flows through a 2 mm channel 3.8 cm in length prior to reaching the point of vaporization. Following the point of vaporization this channel continues for 1.5 cm at a diameter of 2 mm, then expands to a diameter of 4 mm for the remaining 1.0 cm. Following this region the gases expand into a large vacuum chamber maintained at an average pressure of approximately 2×10^{-3} Torr. Following passage through a 5 mm, 55° conical skimmer (Beam Dynamics), the molecular beam enters the ionization region of a reflectron-type time-of-flight mass spectrometer[27] (TOFMS) where the resonant two-photon ionization experiments are conducted.

Initial low resolution vibronic scans were performed using a Nd:YAG-pumped (Quantel, model 581-C) dye laser (Molectron, model DL-II), which was operated on stilbene 420 laser dye (Exciton). The tunable output of this laser was frequency doubled using a β-barium borate crystal ($7\times7\times7$ mm, Skytek) and both the fundamental and the second harmonic of the dye laser output were directed into the TOFMS ionization region. With this arrangement no

problems in spatial or temporal overlap of the excitation (fundamental) or ionization (second harmonic) laser beams could occur, because they were completely coincident in time and space. In a search for the spectrum of a previously unknown molecule this method has the additional advantage that two frequency ranges are scanned simultaneously, and if a transition is found it may subsequently be determined whether the excitation involves the fundamental or the second harmonic radiation. After transitions were located for GaAs in this way, we found that the quality of the spectra could be improved by using excimer laser radiation (Questek, model 2420) as the ionization laser, and that either ArF (193 nm) or KrF (249 nm) radiation could be used in place of the dye laser second harmonic radiation. Since KrF radiation resulted in a lower nonresonant background signal than could be obtained with ArF light, the best spectra were obtained using KrF radiation as the ionization color. This includes all of the spectra shown in this paper.

In addition to low-resolution vibronic scans of GaAs, high-resolution (0.04 cm^{-1}) scans were obtained using an intracavity etalon and accessories (Molectron, Model DL224). The intracavity etalon and diffraction grating were pressure tuned from 0 to 1 atm using SF_6, and the resulting spectra were calibrated using the transmission fringes of a 0.215 cm^{-1} free spectral range etalon. Finally, excited state lifetimes were obtained by time-delayed resonant two-photon ionization, with the resulting profile fitted to an exponential decay.

In the course of these investigations we found it necessary to scan to the blue of stilbene 420 laser dye. After replacing the O-rings in the dye laser with ethylene–propylene, we investigated a number of dyes which lase to the blue of stilbene 420, but which require *p*-dioxane as a solvent. These included DPS, BBO, Bis-MSB, and Exalite 398 (all available from Exciton). Only BBO was found to overlap with the tuning range of stilbene 420. Moreover, its efficiency was only half that of stilbene 420. Further to the blue the dyes DPS and Exalite 398 work well, but this was irrelevant since our spectra were contained within the tuning range of stilbene 420 and BBO. All of the spectra reported here were obtained using either stilbene 420 or BBO.

One final experimental difficulty was a serious fluctuation in signal intensity. In part, this may be due to a preferential loss of As_2 from the laser-heated GaAs surface, leading to a heterogeneous surface composition with domains of GaAs, metallic gallium, and possibly crystalline arsenic. As a result of the rotational recycling of the disk over itself, a varying chemical and topographic environment is presented to the vaporization laser, leading to extreme variations in signal intensity. This effect was quite devastating in the high-resolution scans, in which the dye laser power was reduced one or two orders of magnitude to prevent power broadening of the rotational lines. The reduction in dye laser power was at the expense of the enhancement, making it very difficult to pick out the dye-laser enhanced signal from the fluctuating excimer-only background. Ultimately this problem was overcome by simultaneously recording the Ga_2^+ signal, which results from non-resonant excimer-only photoionization of Ga_2. Experimentally it was found that the fluctuations in GaAs and Ga_2 signals were strongly correlated, and a reasonable GaAs spectrum could be obtained by dividing the GaAs raw data by the Ga_2 signal at every recorded point in the spectrum. This procedure was followed for all of the high-resolution spectra shown below.

III. RESULTS

A. Low-resolution spectra

Figure 1 displays the low-resolution resonant two-photon ionization spectra of $^{69}Ga^{75}As$ and $^{71}Ga^{75}As$ over the spectral range 23 000–24 800 cm^{-1}. The spectrum is generally irregular in appearance, with very different patterns of intensity in the two isotopic modifications. Despite these complexities, vibrational progressions, hot bands originating from $v'' = 1$ and 2, and transition types ($\Omega' \leftarrow \Omega''$) have been assigned, and are indicated on the figure. These assignments have been made possible by the measurement of isotope shifts (thereby permitting a definite vibrational numbering), and by the resolution of rotational structure in the individual subbands (thereby permitting a definite assignment of Ω' and Ω'').

At first sight, the spectrum appears to break into an irregular region to the blue of 23 600 cm^{-1} and a more regular portion to the red of this frequency. The red portion of the spectrum consists of a strong triplet of bands between 23 500 and 23 600 cm^{-1}, with this structure repeated approximately 205 cm^{-1} to the red, and partially repeated again approximately 200 cm^{-1} further to the red. Based on the rapid drop in intensity and the decreasing vibrational interval as one proceeds toward the red, it is clear that the repetitious structure below 23 500 cm^{-1} arises from vibrational hot bands, with a ground state vibrational frequency in the neighborhood of 210 cm^{-1}. Extrapolating this hot band progression to the blue is impossible for the two higher frequency members of the triplet, but the lowest frequency member

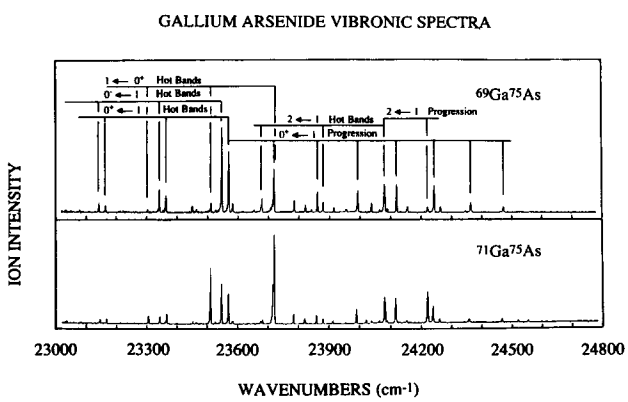

FIG. 1. Low-resolution vibronic spectra of the 409–432 nm band system of $^{69}Ga^{75}As$ and $^{71}Ga^{75}As$. In the text this is identified as a $^3\Pi \leftarrow X\,^3\Sigma^-$ band system. In this figure hot bands and progressions are identified by the values of Ω' and Ω'', as $\Omega' \leftarrow \Omega''$ transitions. This spectrum is a composite of two scans employing stilbene 420 and BBO laser dyes, and has not been corrected for variations in dye laser intensity. As a result, the transitions near 23 900 cm^{-1} appear less intense than they actually are, since this region falls in the dip between the two dye curves.

may be readily extrapolated one more vibrational quantum to give the most intense feature in the $^{71}Ga^{75}As$ spectrum. Accordingly, the features for $^{71}Ga^{75}As$ at 23 544.6, 23 566.7, and 23 716.6 cm^{-1} are assigned as origin subbands, corresponding to different $\Omega' \leftarrow \Omega''$ transitions in a GaAs molecule with nonzero electronic spin, in either Hund's case (a) or case (c).

Upon detailed inspection of the region to the blue of 23 600 cm^{-1}, a vibrational progression with an upper state frequency of about 150 cm^{-1} is found to be built upon the 23 566.7 cm^{-1} origin subband. This progression and hot bands built upon it account for nearly all of the structure to the blue of 23 750 cm^{-1}. No corresponding progression is found to be associated with either the 23 544.6 or 23 716.6 origin subbands.

The strongest of the remaining bands of $^{69}Ga^{75}As$, at 24 078.8 cm^{-1}, exhibits a series of hot bands associated with it, with an interval of 200–205 cm^{-1}. Likewise, one member of a progression in the excited state vibration is observed at 24 219 cm^{-1}. The strong feature at 24 078 cm^{-1} is therefore assigned as another origin subband, making a total of four observed origin subbands. The frequencies and assignments of all observed bands are given in Table I.

B. High-resolution spectra: Identification of the system as $^3\Pi_r \leftarrow X\,^3\Sigma^-$

High-resolution investigations of several vibronic features were undertaken to identify the term symbols involved in the transition, and to measure the GaAs bond length. The origin subbands at 23 544.6 and 23 566.7 cm^{-1} are shown in high resolution (0.04 cm^{-1}) in Figs. 2 and 3. These sub-

TABLE I. Vibronic bands of the $^3\Pi \leftarrow X\,^3\Sigma^-$ system of GaAs.[a]

Assignment		Frequency		Isotope	ν(expt) − ν(calc)		Lifetime (ns)[f]	
$v' \leftarrow v''$	$\Omega' \leftarrow \Omega''$	$^{69}Ga^{75}As$	$^{71}Ga^{75}As$	shift	$^{69}Ga^{75}As$	$^{71}Ga^{75}As$	$^{69}Ga^{75}As$	$^{71}Ga^{75}As$
0–2	0^-–1	23 138.9	23 141.6	− 2.75				
0–2	0^+–1	23 161.4	23 164.4	− 2.98	0.9	0.7		
0–2	1–0^+	23 304.9	23 300.9	− 3.12				116 ± 4
0–1	0^-–1	23 338.4	23 340.3	− 1.95			412 ± 5	125 ± 3
0–1	0^+–1	23 361.6	23 363.4	− 1.73	1.1	1.4	542 ± 55	476 ± 11
2–2	0^+–1	23 445.9	23 447.8	− 1.99	− 1.6	− 0.8		
0–1	1–0^+[b]	23 508.0	23 508.4	− 0.165[c]			22 ± 33	123 ± 6
0–0	0^+–0^+	23 523.7	23 523.8	− 0.16				
0–0	0^-–1[b]	23 544.7	23 544.6	− 0.272[c]			358 ± 10	118 ± 36
0–0	0^+–1[b]	23 566.8	23 566.7	− 0.210[c]	− 0.8	− 0.9	617 ± 23	571 ± 6
3–2	0^+–1	23 579.3	23 579.6	− 0.172[c]	− 3.0	− 3.0	375 ± 27	331 ± 19
2–1	0^+–1	23 647.7	23 645.9	1.79	0.3	− 1.0		
1–0	0^+–0^+	23 671.2	23 671.0	0.21			225 ± 178[e]	174 ± 116[e]
0–2	2–1	23 673.9	23 676.7	− 2.86			225 ± 178[e]	174 ± 116[e]
1–0	0^+–1[b]	23 713.9	23 713.1	0.843[c]	0.0	0.2	59 ± 9	185 ± 38
0–0	1–0^+[b]	g	23 716.6	···			d	133 ± 4
3–1	0^+–1	23 780.4	23 779.5	0.95	− 1.8	− 1.3	290 ± 304	283 ± 153
2–0	0^+–0^+	23 815.5	23 815.1	0.38			328 ± 75	96 ± 36
5–2	0^+–1	23 836.1	23 835.8	0.84	1.5	2.5		
2–0	0^+–1[b]	23 855.9	23 853.7	1.770[c]	1.4	1.2	112 ± 15	96 ± 10
0–1	2–1	23 874.0	23 875.8	− 1.92			308 ± 37	
4–1	0^+–1	23 910.9	23 908.7	1.80	− 0.4	− 0.4	330 ± 119	233 ± 40
6–2	0^+–1	23 955.5	23 951.6	2.64	3.4	1.4		
3–0	0^+–1	23 990.2	23 987.2	2.96	0.9	0.7	479 ± 39	
5–1	0^+–1	24 036.1	24 033.5	2.58	1.5	1.9		
7–2	0^+–1	24 062.8	24 060.5	2.29	− 1.1	− 0.8		
0–0	2–1[b]	24 078.8	24 078.8	− 0.222[c]			310 ± 42	247 ± 26
4–0	0^+–1	24 117.9	24 113.7	3.99	− 0.5	− 1.0	255 ± 138	340 ± 153
6–1	0^+–1	24 153.8	24 149.9	3.90	1.7	1.5		
1–0	2–1[b]	24 219.1	24 219.2	0.827[c]			10 ± 1	62 ± 27
5–0	0^+–1	24 240.4	24 236.5	3.92	− 1.3	− 0.7		
7–1	0^+–1	24 261.4	24 257.4	3.96	− 2.4	− 2.2		
6–0	0^+–1	24 360.9	24 355.8	5.10	1.7	1.7		
7–0	0^+–1	24 469.5	24 464.0	5.52	− 1.4	− 1.2		

[a] All numerical values except for lifetimes are given in cm^{-1}, with an estimated uncertainty in absolute frequency of ± 10 cm^{-1}. The uncertainty in relative frequencies is much less, probably below 3 cm^{-1}.

[b] Assignment of Ω' and Ω'' established by high-resolution scans, although this cannot distinguish $\Omega' = 0^+$ from $\Omega' = 0^-$.

[c] Isotope shift measured in high-resolution scans; estimated accuracy is ± 0.02 cm^{-1}. In the remaining entries the isotope shifts were measured in low resolution scans, giving estimated errors of 0.5 cm^{-1}.

[d] Lifetime is too fast to measure.

[e] Lifetime measurements are ambiguous due to overlapping bands.

[f] Uncertainties in lifetime measurements are quoted as one standard deviation in the nonlinear least-squares fit. Repetitive measurements on the same band, however, suggest that a more accurate estimate would be ± 10% of the fitted lifetime.

[g] Despite repeated efforts, this band was never observed for $^{69}Ga^{75}As$. It should have a short lifetime and may be obscured by the nearby 1–0 band of the $\Omega' = 0^+ \leftarrow \Omega'' = 1$ transition as well.

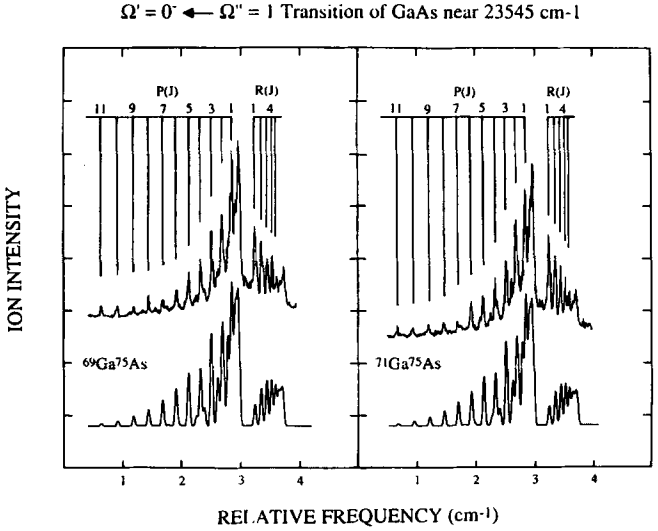

FIG. 2. High-resolution spectrum of the $v' = 0 \leftarrow v'' = 0$ band of the $^3\Pi_0 \leftarrow X\,^3\Sigma_1^-$ transition of GaAs, located near 23 545 cm^{-1}. A comparison with the spectral simulation shown below demonstrates that the experimental intensity pattern is generally well-reproduced in the simulation.

bands have a strong P branch, a definite Q branch, and a rather weak R branch. Both are quite similar in appearance, having an obvious gap between the Q branch and the first R line, and showing the R branch coming to a head within 1 cm^{-1} of its first line. Detailed analysis of these subbands shows that both are $\Omega' = 0 \leftarrow \Omega'' = 1$ transitions, for which the first lines are $R(1)$, $Q(1)$, and $P(1)$. This assignment is consistent with the gap between the Q and R branches, since $R(0)$ is missing. It is also consistent with the intensity distribution in the branches, since a $\Delta\Omega = -1$ transition normally shows a strong P branch and a weak R branch. The presence of *two* $\Omega' = 0 \leftarrow \Omega'' = 1$ subbands demonstrates that the upper state possesses both $\Omega = 0^+$ and $\Omega = 0^-$ components. On this basis the upper state could be $^3\Pi$, $^5\Pi$, $^5\Delta$, or a term of higher Λ or S, but cannot be a Σ state or a singlet.

Figure 4 displays a high-resolution scan over the 23 508 cm^{-1} subband for both $^{69}Ga^{75}As$ and $^{71}Ga^{75}As$. Although we believed this to be an origin subband when it was first scanned at high resolution, it is now fairly clear that it is vibrationally a 0–1 hot band. This subband shows a very different rotational structure than that found for the $\Omega' = 0 \leftarrow \Omega'' = 1$ bands exhibited in Figs. 2 and 3. The R branch is more intense than the P branch, and there is no missing line between the Q branch and the first R line. The presence of an $R(0)$ line demonstrates that $\Omega'' = 0$, while the presence of a Q branch implies a perpendicular transition, giving $\Omega' = 1 \leftarrow \Omega'' = 0$. There is no evidence of Λ-type doubling in the lower state, implying that there is only one $\Omega'' = 0$ component. This in turn identifies the lower state as a Σ state, with $^3\Sigma$, $^5\Sigma$,... as the only possibilities. As in Figs. 2 and 3, a simulated spectrum is shown in the lower panel.

A rotationally resolved scan of the last of the subband systems, the origin subband at 24 078.8 cm^{-1}, is shown in Fig. 5. This subband again shows a gap between the intense Q branch and the first R line, as do the $\Omega' = 0 \leftarrow \Omega'' = 1$ transitions of Figs. 2 and 3. The subband shown in Fig. 5, however, shows an intense R branch and a comparatively weak P branch. This is indicative of a $\Delta\Omega = +1$ transition. Detailed analysis and spectral simulations demonstrate that this subband is an $\Omega' = 2 \leftarrow \Omega'' = 1$ transition, for which the first lines are $R(1)$, $Q(2)$, and $P(3)$. The general pattern of intensities is well reproduced by the spectral simulation shown in the lower panel.

All of the observed transitions are perpendicular transitions, with $\Delta\Omega = \pm 1$. In Hund's case (a) this implies that $\Delta\Lambda = \pm 1$. Having determined that $\Lambda'' = 0$, the only possibility is that $\Lambda' = 1$, giving a $\Pi \leftarrow \Sigma$ transition. Furthermore, $^1\Pi \leftarrow {}^1\Sigma$ is ruled out by the observation of multiplet splittings, but $^3\Pi \leftarrow {}^3\Sigma$, $^5\Pi \leftarrow {}^5\Sigma$, and higher multiplicity transi-

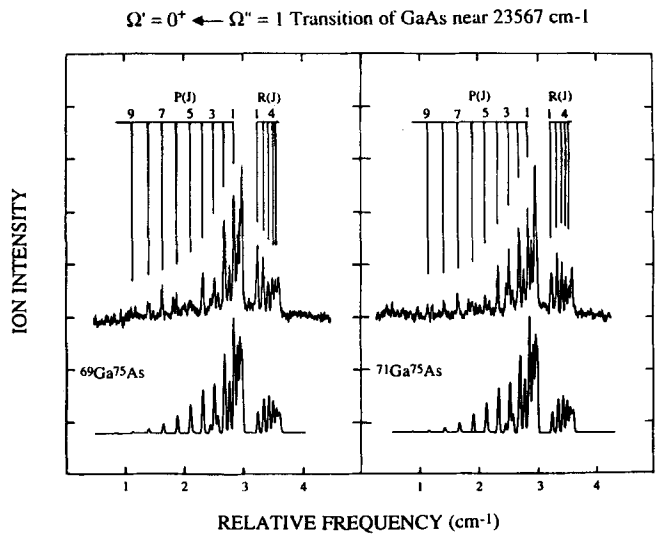

FIG. 3. High-resolution spectrum of the $v' = 0 \leftarrow v'' = 0$ band of the $^3\Pi_0 \leftarrow X\,^3\Sigma_1^-$ transition of GaAs, located near 23 567 cm^{-1}. The pattern of features is nearly identical to that observed for the $^3\Pi_0 \leftarrow X\,^3\Sigma_1^-$ transition shown in Fig. 2, and is well reproduced by the spectral simulation shown below.

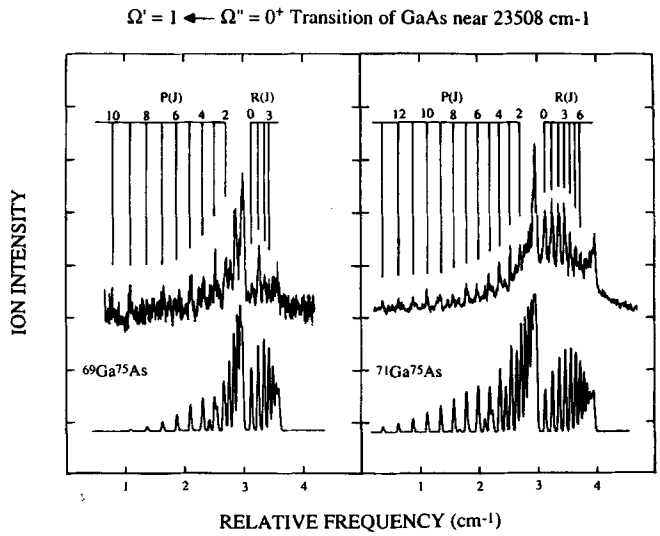

FIG. 4. High-resolution spectrum of the $v' = 0 \leftarrow v'' = 1$ hot band of the $^3\Pi_1 \leftarrow X\,^3\Sigma_0^-$ transition of GaAs, located near 23 508 cm^{-1}. The presence of the $R(0)$ line identifies $\Omega'' = 0$, and the presence of a Q branch proves that the transition is an $\Omega' = 1 \leftarrow \Omega'' = 0$ transition.

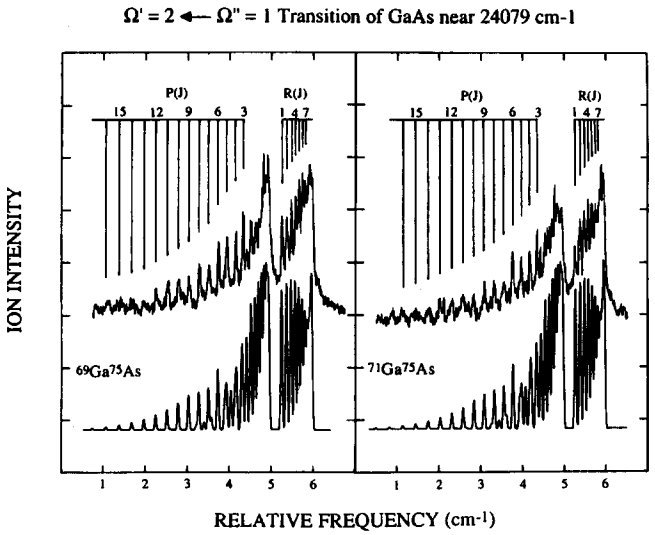

FIG. 5. High-resolution spectrum of the $v' = 0 \leftarrow v'' = 0$ band of the $^3\Pi_2 \leftarrow X\,^3\Sigma_1^-$ transition of GaAs, located near 24 079 cm^{-1}. The lack of an $R(0)$ line and the presence of $R(1)$ identify $\Omega'' = 1$, while the high intensity of the R branch implies a $\Delta\Omega = +1$ transition, thereby confirming the assignment as $\Omega' = 2 \leftarrow \Omega'' = 1$.

tions are still potential candidates for consideration. Of these choices, the assignment $^3\Pi \leftarrow X\,^3\Sigma$ is by far the most reasonable. Higher multiplicity transitions such as $^5\Pi \leftarrow {}^5\Sigma$ would be expected to give additional subbands originating from $\Omega'' = 2$, which are not observed. In addition, given four p electrons to be distributed in the molecule, the most favorable bonding arrangements would be to place these in σ or π bonding orbitals as $\sigma^2\pi^2(^3\Sigma^-)$, $\sigma\pi^3(^3\Pi)$, or $\pi^4(^1\Sigma^+)$. The ground state of GaAs has been predicted[23,25] to be $^3\Sigma^-$, and the analogous $^3\Sigma_g^-$ state is known[8,9] to be the ground state of Si_2. Based on these considerations, we assign the observed band system as $^3\Pi \leftarrow X\,^3\Sigma^-$. This assignment gives $\Omega' = 1 \leftarrow \Omega'' = 0^+$, $\Omega' = 0^+ \leftarrow \Omega'' = 1$, $\Omega' = 0^- \leftarrow \Omega'' = 1$, and $\Omega' = 2 \leftarrow \Omega'' = 1$ subbands in case (a), all of which are observed.

The precisely known[33,34] absorption spectrum of I_2 is unfortunately not useful for calibration above 20 000 cm^{-1}, so the major impediment to the precise measurement of rotational constants for GaAs is the uncertainty in the free spectral range of the monitoring etalon. This places an uncertainty of approximately $\pm 2\%$ on all of our measured rotational constants. Nevertheless, we have analyzed the bands shown in Figs. 2–5 (and several others) by fitting individual rotational lines to the formula

$$\nu = \nu_0 + B'J'(J'+1) - B''J''(J''+1). \qquad (1)$$

The rotational constants obtained in these band-by-band fits are given in Table II. These are combined with vibrational constants and electronic energies in Table III.

C. Spin–orbit structure of the $X\,^3\Sigma^-$ and $^3\Pi_r$ states

The identification of the origin subbands associated with the $\Omega' = 2 \leftarrow \Omega'' = 1$ and the two $\Omega' = 0 \leftarrow \Omega'' = 1$ transitions allow the term energies of the $^3\Pi_2$ and the two $^3\Pi_0$ substates to be measured relative to the $^3\Sigma_1^-$ substate. Likewise, the $\Omega' = 1 \leftarrow \Omega'' = 0^+$ origin subband gives the energy of the $^3\Pi_1$ level relative to the $^3\Sigma_{0^+}^-$ component of the ground state. These two energy schemes, however, cannot be easily related since there are no transitions allowed in Hund's case (a) which can couple a substate from the first set ($^3\Pi_2$, $^3\Pi_{0^+}$, $^3\Pi_{0^-}$, $^3\Sigma_1^-$) to a substate from the second set ($^3\Pi_1$, $^3\Sigma_{0^+}^-$). In other molecules a breakdown of Hund's case (a) toward case (c) has sometimes permitted forbidden subbands such as $\Omega' = 0^+ \leftarrow \Omega'' = 0^+$ or $\Omega' = 1 \leftarrow \Omega'' = 1$ to be observed,

TABLE II. Measured rotational constants of GaAs.[a]

Band assignment		B' (cm^{-1})		B'' (cm^{-1})		N[b]		Δ (cm^{-1})[c]	
$v' \leftarrow v''$	$\Omega' \leftarrow \Omega''$	$^{69}Ga^{75}As$	$^{71}Ga^{75}As$	$^{69}Ga^{75}As$	$^{71}Ga^{75}As$	$^{69}Ga^{75}As$	$^{71}Ga^{75}As$	$^{69}Ga^{75}As$	$^{71}Ga^{75}As$
0–0	$0^- \leftarrow 1$	0.066 75	0.066 13	0.073 43	0.072 65	20	20	0.007	0.007
		± 0.000 24	± 0.000 25	± 0.000 20	± 0.000 21				
0–0	$0^+ \leftarrow 1$	0.065 81	0.064 60	0.073 48	0.072 20	19	18	0.007	0.005
		± 0.000 27	± 0.000 18	± 0.000 25	± 0.000 15				
1–0	$0^+ \leftarrow 1$	0.065 23	0.064 76	0.073 44	0.072 84	15	12	0.005	0.008
		± 0.000 26	± 0.000 47	± 0.000 25	± 0.000 39				
2–0	$0^+ \leftarrow 1$	0.064 20	0.065 10	0.073 42	0.074 41	13	8	0.006	0.010
		± 0.000 35	± 0.002 10	± 0.000 26	± 0.001 46				
0–0	$2 \leftarrow 1$	0.069 00	0.067 69	0.074 17	0.072 80	22	19	0.007	0.006
		± 0.000 17	± 0.000 18	± 0.000 14	± 0.000 16				
1–0	$2 \leftarrow 1$	···	0.067 04	···	0.072 60	···	15	···	0.010
			± 0.000 31		± 0.000 25				
0–1	$1 \leftarrow 0^+$	0.066 21	0.066 53	0.074 30	0.071 44	9	26	0.003	0.008
		± 0.000 34	± 0.000 15	± 0.000 27	± 0.000 14				
0–0	$1 \leftarrow 0^+$	···	0.066 16	···	0.071 28	···	28	···	0.006
			± 0.000 11		± 0.000 11				

[a] Quoted uncertainties are one standard deviation in the least-squares fit, and do not reflect the $\pm 2\%$ error which results from imprecise knowledge of the monitor etalon free spectral range.
[b] N is the number of rotational lines used in the least-squares fit.
[c] Δ is the root mean square error in the least-squares fit.

TABLE III. Molecular constants of the ground and excited states of GaAs.[a]

State	Constant	$^{69}Ga^{75}As$	$^{71}Ga^{75}As$
$^3\Pi_2$	T_0	24 087.80	24 087.80
	$\Delta G'_{1/2}$	140.30	140.40
	B'_0	0.069 00 ± 0.001 38	0.067 69 ± 0.001 35
	B'_1		0.067 04 ± 0.001 34
	r'_0	2.609 ± 0.026 Å	2.614 ± 0.026 Å
$^3\Pi_1$	T_0	23 760.40	23 759.50
	B'_0	0.066 21 ± 0.001 32	0.066 29 ± 0.001 33
	r'_0	2.663 ± 0.027 Å	2.642 ± 0.026 Å
$^3\Pi_{0+}$	T_0	23 567.58 ± 1.07	23 567.60 ± 0.96
	ω'_e	152.13 ± 0.70	151.01 ± 0.62
	$\omega'_e x'_e$	2.89 ± 0.08	2.85 ± 0.08
	B'_0	0.065 81 ± 0.001 32	0.064 60 ± 0.001 29
	B'_1	0.065 23 ± 0.001 30	0.064 76 ± 0.001 30
	B'_2	0.064 20 ± 0.001 28	0.065 10 ± 0.001 30
	α'_e	0.000 81	
	B'_e	0.066 29 ± 0.001 85	
	r'_0	2.671 ± 0.027 Å	2.676 ± 0.027 Å
	r'_e	2.662 ± 0.027 Å	
$^3\Pi_{0-}$	T_0	23 544.70	23 544.60
	B'_0	0.066 75 ± 0.001 34	0.066 13 ± 0.001 32
	r'_0	2.652 ± 0.026 Å	2.645 ± 0.026 Å
$X\,^3\Sigma^-_{0+}$	T_0	43.10	42.90
	ω''_e	215.50	208.90
	$\omega''_e x''_e$	3.10	0.35
	B''_0		0.071 28
	B''_1	0.074 30	0.071 44
	r''_0		2.548 ± 0.025 Å
$X\,^3\Sigma^-_1$	T_0	0	0
	ω''_e	214.26 ± 2.55	213.02 ± 2.30
	$\omega''_e\omega''_e$	3.58 ± 0.85	3.69 ± 0.76
	B''_0	0.073 75 ± 0.001 48	0.072 56 ± 0.001 45
	r''_0	2.523 ± 0.025 Å	2.525 ± 0.025 Å
	B''^{b}_e	0.074 21 ± 0.001 48	0.073 02 ± 0.001 46
	α''^{b}_e	0.000 92	0.000 92
	r''^{b}_e	2.516 ± 0.025 Å	2.517 ± 0.025 Å

[a] All constants are given in cm^{-1}, except for bond lengths which are given in Angstroms. Uncertainties in rotational constants are ± 2% and uncertainties in bond lengths are ± 1% based on the estimated uncertainty in the monitor etalon free spectral range (± 2%). Uncertainties in T_0, ω_e, and $\omega_e x_e$ are one standard deviation (1σ) in the least-squares fit.

[b] Estimated from the Pekeris relationship, $\alpha_e = 6(\omega_e x_e B_e^3)^{1/2}/\omega_e - 6B_e^2/\omega_e$ (Ref. 32).

thereby allowing the term energies of all the spin–orbit components to be known relative to the same zero of energy.[35] With such a possibility in mind, we have carefully searched for weak unexplained vibronic features in the low-resolution spectrum.

As listed in Table I, a weak series of features has been found, consisting of transitions at 23 524, 23 671, and 23 815 cm^{-1}. The intervals between these features, 147.5 and 144.3 cm^{-1}, closely match the intervals between the 0–0, 1–0, and 2–0 vibrational bands of the progression-forming $\Omega' = 0 \leftarrow \Omega'' = 1$ system, which are 147.1 and 142.0 cm^{-1} (all quoted for the $^{69}Ga^{75}As$ isotopic species). Accordingly, it would seem that the weak transitions at 23 524, 23 671, and 23 815 cm^{-1} correspond to upper state vibrational levels with $v' = 0$, 1, and 2, respectively. As discussed in Sec. III D below, we believe that the progression-forming $\Omega' = 0$ state is the $^3\Pi(\Omega' = 0^+)$ substate, and that the $^3\Pi_2$, $^3\Pi_1$, and $^3\Pi_{0^-}$ substates predissociate for $v' \geqslant 1$. This Ω-selective predissociation then explains the absence of any $v' \geqslant 1$ bands in the low-resolution spectrum of the $\Omega' = 2$, 1, or 0^- states (with the exception of the $v' = 1$, $\Omega' = 2$ level, which predissociates slowly enough to be observed). Given that the only two subbands forbidden in case (a) which become allowed in case (c) are the $\Omega' = 0^+ \leftarrow \Omega'' = 0^+$ and $\Omega' = 1 \leftarrow \Omega'' = 1$ subbands, and that no excited vibrational levels of the $\Omega' = 1$ substate have been observed, the very weak set of bands at 23 524, 23 671, and 23 815 cm^{-1} must correspond to the forbidden $\Omega' = 0^+ \leftarrow \Omega'' = 0^+$ subband. The only alternate possibility, that these are hot bands of the $\Omega' = 0^+ \leftarrow \Omega'' = 1$ system, is readily dismissed since the $v' - 1$ and $v'' - 2$ hot band progressions of this system have been located, and the very weak set of bands does not belong to them. Neither is it consistent with a $v' - v''$ progression with $v'' > 1$.

Having located the forbidden $\Omega' = 0^+ \leftarrow \Omega'' = 0^+$ subband, the complete table of term energies follows. As listed in Table III and depicted in Fig. 6, the term energies are given relative to the zero-point level of the $^3\Sigma_1^-$ substate, which lies 43 cm^{-1} below the $^3\Sigma^-_{0^+}$ substate. This splitting is rather large, and is in the opposite direction of that normally observed for a π^2, $^3\Sigma^-$ ground state (such as SO, S_2, SeO, SeS, Se_2, TeO, TeS, TeSe, and Te_2).[7] In all of these molecules

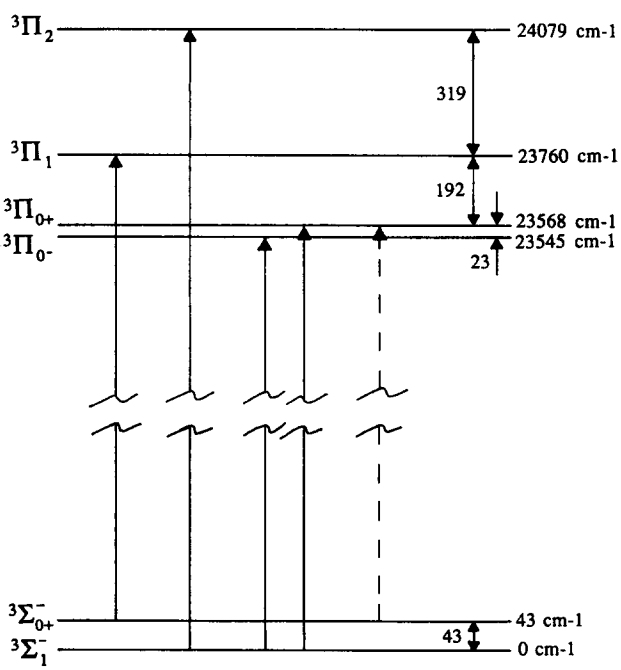

FIG. 6. Term energies of the vibrationless levels of the $X\,^3\Sigma_1^-$, $X\,^3\Sigma^-_{0^+}$, $^3\Pi_0$, $^3\Pi_{0^-}$, $^3\Pi_1$, and $^3\Pi_2$ states, as determined from this work. Solid lines indicate the strong transitions which are allowed in Hund's case (a). The dashed line indicates the very weak $\Omega' = 0^+ \leftarrow \Omega'' = 0^+$ transition, which becomes allowed as Hund's case (c) is approached. Observation of this very weak transition has allowed the construction of this complete term energy diagram.

the π^2, $^3\Sigma^-$ state is split into $\Omega = 0^+$ and $\Omega = 1$ components by off-diagonal spin–orbit interaction with the low-lying π^2, $^1\Sigma^+$ state.[36] Such an interaction will always lead to the displacement of the $^3\Sigma^-(\Omega = 0^+)$ substate below the $^3\Sigma^-(\Omega = 1)$ component. In GaAs, on the other hand, we observe a splitting of the $^3\Sigma^-$ substates in which the $^3\Sigma_1^-$ component lies below the $^3\Sigma_{0^-}^-$ component. Obviously this cannot be explained by the same second-order spin–orbit interaction which is invoked for the chalcogen dimers, and another mechanism for this splitting must be found.

In contrast to the diatomic chalcogens, in which all of the $\sigma^2\pi^4\pi^{*2}$ molecular terms ($^3\Sigma^-$, $^1\Sigma^+$, and $^1\Delta$) correlate to separated ground state atoms, only the $^3\Sigma^-$ term of the $\sigma^2\pi^2$ configuration of GaAs can correlate to separated ground state gallium ($4s^24p$, $^2P^0$) and arsenic ($4s^24p^3$, $^4S^0$) atoms. The $^1\Sigma^+$ state, which is the dominant perturber of the $X\,^3\Sigma^-$ ground state of the diatomic chalcogens, correlates to a ground state gallium atom ($4s^24p$, $^2P^0$) interacting with an excited state arsenic atom ($4s^24p^3$, $^2D^0$). This separated atom limit lies more than 10 000 cm^{-1} above the ground state separated atoms,[37] thereby making its influence less important in GaAs than in the chalcogen dimers. On the other hand, electronic structure calculations for diatomic GaAs show the $\sigma\pi^3$, $^1\Pi$ state of GaAs lying below the $\sigma^2\pi^2$, $^1\Sigma^+$ state.[23,25] Accordingly, we propose that the observed splitting between the $X\,^3\Sigma_1^-$ and $X\,^3\Sigma_{0^-}^-$ components is the result of a stronger second-order spin–orbit interaction between the $\sigma\pi^3$, $^1\Pi$ ($\Omega = 1$) and $\sigma^2\pi^2$, $^3\Sigma^-$ ($\Omega = 1$) substates than occurs between the $\sigma^2\pi^2$, $^1\Sigma^+$ ($\Omega = 0^+$) and $\sigma^2\pi^2$, $^3\Sigma^-$ ($\Omega = 0^+$) substates. As a result the $^3\Sigma_1^-$ substate is displaced to lower energy than the $^3\Sigma_{0^-}^-$ substate.

D. Predissociation in the excited $^3\Pi_r$ state of GaAs

The lifetimes measured for individual vibronic levels of the GaAs $^3\Pi_r$ excited state (see Table I) show wide fluctuations as functions of v', Ω', and isotopic composition, giving values ranging from $\tau = 600$ ns ($v' = 0$, $\Omega' = 0^+$, either isotope) to $\tau = 10$ ns ($v' = 1$, $\Omega' = 2$, $^{69}Ga^{75}As$). The apparent differences in spectral intensity found for the two isotopic forms (as shown in Fig. 1) are a direct result of the differing lifetimes of the excited state for these two species. This occurs because a substantial fraction of the molecules excited to a short-lived state may decay prior to photoionization, resulting in a reduced ion signal for a short-lived state as compared to that for a long-lived state. This is evident in Fig. 1, where the 0–0 and 0–1 bands of the $\Omega' = 1 \leftarrow \Omega'' = 0^+$ system are much weaker for $^{69}Ga^{75}As$ than for $^{71}Ga^{75}As$, because of the much shorter lifetime of the former species ($\tau = 22$ ns) as compared to the latter ($\tau = 128$ ns). The shortened excited state lifetimes in certain vibronic levels are attributed to predissociation in the excited $^3\Pi_r$ state.

As is evident from Table I, no transitions are found which terminate on $v' > 1$ for $\Omega' = 2$. In addition, no transitions are found terminating on $v' > 0$ for $\Omega' = 1$ and for one $\Omega' = 0$ substate (designated as 0^- in Table I), while a long progression (up to $v' = 7$) is found for the other $\Omega' = 0$ substate (designated as 0^+ in Table I). Thus, rapid predissociation sets in at low v' values for $\Omega' = 2,1$, and for one of the $\Omega' = 0$ substates, while the second $\Omega' = 0$ substate escapes this predissociation unscathed. A consistent mechanism for this predissociation must explain the Ω selectivity of the dissociation process. As described in Sec. III C, a characteristic feature of Σ states is that they possess either an $\Omega = 0^+$ or $\Omega = 0^-$ component, but not both. Thus a predissociation mechanism involving an unbound Σ state would affect only one of the $\Omega' = 0$ components, leaving the other unaffected. To successfully predissociate the $\Omega' = 2,1$, and one $\Omega' = 0$ component, the unbound state responsible for the process must be either $^5\Sigma^-$ (possessing $\Omega = 0^-,1$, and 2 components) or $^5\Sigma^+$ (possessing $\Omega = 0^+,1$, and 2 components). Of these two possibilities, $^5\Sigma^+$ may be discarded, since the first separated atom limit capable of producing a $^5\Sigma^+$ state (Ga $4s4p^2$, ^4P + As $4s^24p^3$, $^4S^0$) lies 38 000 cm^{-1} above ground state atoms.[37] This is simply too high in energy to predissociate states observed near 24 000 cm^{-1}.

A $^5\Sigma^-$ state, however, arises from the ground states of the separated atoms (Ga $4s^24p$, $^2P^0$ + As $4s^24p^3$, $^4S^0$) and is very likely the cause of the observed predissociation process. This state differs from the $X\,^3\Sigma^-$ ground state of GaAs by coupling the $p\sigma$ electron of gallium to the $p\sigma$ electron of arsenic to give $S = 1$, so that the molecular orbital configuration is $\sigma\sigma^*\pi^2$ ($^5\Sigma^-$) instead of $\sigma^2\pi^2$ ($X\,^3\Sigma^-$). As a result, the $^5\Sigma^-$ state possesses a net σ bond order of zero, and has only weak bonding contributions from the π^2 configuration, at best. This state is essentially repulsive, and presumably crosses the $^3\Pi$ upper state slightly above its potential energy minimum. Spin–orbit interactions then couple the $^3\Pi_{0^-}$, $^3\Pi_1$, and $^3\Pi_2$ substates to the $^5\Sigma_{0^-}$, $^5\Sigma_1$, and $^5\Sigma_2$ substates, respectively, thereby predissociating the higher vibrational levels of the $^3\Pi_{0^-}$, $^3\Pi_1$, and $^3\Pi_2$ components. Under this proposed mechanism the $^3\Pi_{0^+}$ component cannot be predissociated, and for this reason the $\Omega' = 0^+$ component is assigned as the progression-forming substate of the excited $^3\Pi$ state. A schematic set of potential energy curves illustrating the predissociation mechanism is shown in Fig. 7.

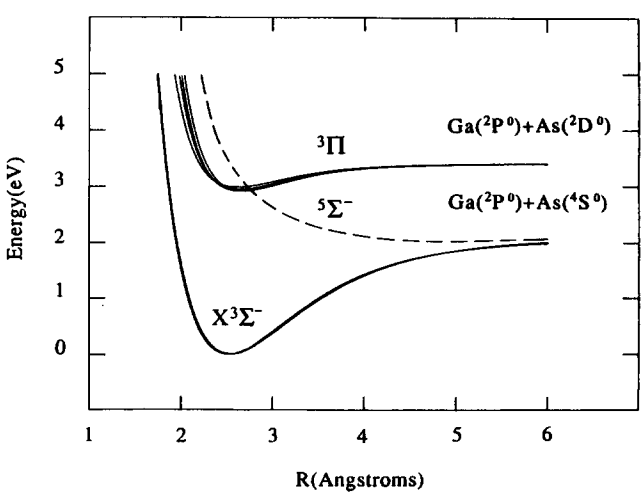

FIG. 7. Potential energy curves of the $X\,^3\Sigma^-$ and $^3\Pi$ states, as determined from this work. The $^5\Sigma^-$ state which is postulated to cause predissociation in the $^3\Pi_0$, $^3\Pi_1$, and $^3\Pi_2$ states is indicated by the dashed line.

An independent verification that the progression-forming substate is described by $\Omega' = 0^+$ rather than $\Omega' = 0^-$ results from the observation of the very weak set of subbands which are forbidden in Hund's case (a). As discussed in Sec. III C, the only subbands which are forbidden in case (a) but become allowed in case (c) are the $\Omega' = 1 \leftarrow \Omega'' = 1$ and $\Omega' = 0^+ \leftarrow \Omega'' = 0^+$ subbands. Since vibronic levels of the $\Omega' = 1$ substate predissociate too rapidly to be observed above $v' = 0$, the observed weak progression cannot be the $\Omega' = 1 \leftarrow \Omega'' = 1$ subsystem, and must be due to the $\Omega' = 0^+ \leftarrow \Omega'' = 0^+$ subsystem. Thus the progression-forming $\Omega' = 0$ substate must be of $\Omega' = 0^+$ symmetry, and the assignment of upper state $\Omega' = 0^\pm$ components is quite definite.

E. Ionization potential and dissociation energy of GaAs

The various combinations of ionization lasers used successfully to generate the spectrum of GaAs allow the ionization potential, IP(GaAs), to be bracketed. The observation of the spectrum with ArF radiation as the photoionization laser implies IP(GaAs) > 6.42 eV, while the observation of the 0–0 band of the $\Omega' = 0^- \leftarrow \Omega' = 1$ subsystem with KrF radiation implies IP(GaAs) < 7.92 eV. Together, these observations provide IP(GaAs) $= 7.17 \pm 0.75$ eV, where the large uncertainty could be narrowed by further experiments employing other photoionization lasers, or by direct one-photon ionization methods. No previous measurements of the ionization potential of GaAs appear to have been made. The result that the GaAs ionization potential is greater than that of atomic gallium (6.00 eV)[37] implies that the GaAs bond strength is decreased when it is ionized to form $GaAs^+$.

The dissociation energy $D_0(GaAs)$ has been previously measured by Knudsen effusion mass spectrometry, giving $D_0(GaAs) = 2.17 \pm 0.01$ eV by the third-law method.[38] As is well known, this method employs the statistical mechanical expression for a gas-phase chemical equilibrium in combination with measured values of the equilibrium constant to obtain bond strengths. In the process, one must assume bond lengths, vibrational frequencies, and the energies of low-lying excited electronic states to calculate the partition functions which are needed for the statistical expression for the equilibrium constant. Errors can arise, since only rarely is all of this information available. Using the measured equilibrium constants[38] for the process

$$Ga(g) + 1/2\ As_2(g) \rightleftarrows GaAs(g),$$

the well-known spectroscopic parameters for As_2 (Ref. 7, $r_e = 2.1026$ Å, $\omega_e = 429.5\ cm^{-1}$, $D_0(As_2) = 3.96$ eV), and our measured spectroscopic constants for GaAs (see Table III), we have recalculated $D_0(GaAs)$ by the third-law method. The resulting value, $D_0(GaAs) = 2.09 \pm 0.02$ eV is somewhat reduced from the previously accepted value. This bond strength is reduced further to $D_0(GaAs) = 2.03 \pm 0.02$ eV or 2.06 ± 0.02 eV if additional low-lying states calculated by Balasubramanian[23] or Meier *et al.*[25] are included in the partition function. Assuming that the Knudsen effusion measurements (which were obtained using an unconventional double oven apparatus)[38] are valid, a conservative revised estimate of the bond strength of GaAs is then $D_0(GaAs) = 2.06 \pm 0.05$ eV.

In addition to this estimate of the bond strength of ground state GaAs, we may estimate the well depth for electronically excited GaAs ($^3\Pi$) by the relationship[32] $D_e = \omega_e^2/(4\omega_e x_e)$, which is valid for Morse potentials. Since both ω_e and $\omega_e x_e$ are well-determined for the $^3\Pi_{0^+}$ state where $v' = 0$ to 7 have been observed, the resulting value of D_e (GaAs, $^3\Pi$) will be reasonable if the assumption of a Morse-like potential curve is not too far wrong. Adopting this procedure, we obtain D_e (GaAs, $^3\Pi$) $= 0.25$ eV, indicating that the excited $^3\Pi$ state is only weakly bound. Furthermore, this information may be combined with the ground state bond strength $D_0(GaAs) = 2.06 \pm 0.05$ eV and the $^3\Pi_{0^+} \leftarrow X\,^3\Sigma_1$ excitation energy, $T_0 = 23\,567.58\ cm^{-1}$, to obtain the energy of the separated atom limit to which the excited $^3\Pi$ state dissociates. This simple calculation predicts that the $^3\Pi$ state dissociates to a separated atom limit lying $8950\ cm^{-1}$ above ground state atoms. The lowest excited separated atom limits for Ga + As are $^2P^0 + {}^2D^0$ at $10\,786\ cm^{-1}$, $^2P^0 + {}^2P^0$ at $18\,494\ cm^{-1}$, and $^2S + {}^4S^0$ at $24\,238\ cm^{-1}$, from which we conclude that the excited $^3\Pi$ state dissociates to a ground state $4s^24p$, $^2P^0$ gallium atom and an excited $4s^24p^3\,{}^2D^0$ arsenic atom, as is indicated in Fig. 7. Since a $^3\Pi$ state also arises from the interaction of two ground state atoms, the band system we observe must correspond to the second excited $^3\Pi$ state (or possibly to the third or fourth, since three $^3\Pi$ states derive from the $^2P^0 + {}^2D^0$ separated atom limit).

IV. DISCUSSION

The spectroscopic results described in the previous section are in excellent agreement with the most recent *ab initio* calculation on GaAs,[25] and are in general agreement with the previous calculation by Balasubramanian.[23] These two calculations both correctly predict a $^3\Sigma^-$ ground state for GaAs, but predict bond lengths which are 0.05[25] or 0.25 Å[23] longer than experiment, respectively. The calculated ground state vibrational frequencies are 5%[25] or 23%[23] lower than experiment, and the calculated bond strengths are 22%[25] or 43%[23] too low as well. Such errors in bond strengths are not unexpected, since it is well known that bond strengths are among the most difficult properties to compute with accuracy. A more recent calculation by Balasubramanian[41] employing a revised effective core potential for gallium leads to greatly improved bond lengths, vibrational frequencies, and excitation energies, as compared to the measured values provided here.

The recent *ab initio* MRD-CI investigation by Meier *et al.*[25] offers some insight into the excited $^3\Pi$ state observed in this investigation. These authors calculate three excited $^3\Pi$ states, the lowest of which is a candidate for the ground state ($\sigma\pi^3$, $^3\Pi$), and lies much lower than the upper state of our band system. The next two $^3\Pi$ states correlate to the Ga $4s^24p$, $^2P^0$ + As $4s^24p^3$, $^3D^0$ separated atom limit, and lie closer to the region probed in this study. The $2^3\Pi$ state calculated by Meier *et al.*[25] lies at an electronic energy of 17 700 cm^{-1}, has a bond length of 3.12 Å, and a vibrational fre-

quency of 132 cm^{-1}. The $3^3\Pi$ state lies at 21 600 cm^{-1}, has a bond length of 2.70 Å, and a vibrational frequency of 150 cm^{-1}. This latter $^3\Pi$ state compares very favorably with the upper state of our band system, which lies at 23 545 cm^{-1}, with $r_e = 2.66$ Å, and $\omega_e = 152$ cm^{-1}. Based on the agreement between the calculated $3^3\Pi$ state and our observed $^3\Pi$ state, the observed band system is assigned as $3^3\Pi \leftarrow X\,^3\Sigma^-$. These authors also calculate the $\sigma\sigma^*\pi^2$, $^5\Sigma^-$ state, and find that it crosses both the $2^3\Pi$ and $3^3\Pi$ states slightly above their potential minima, confirming our analysis of the predissociation observed in the $3^3\Pi$ state.

The experimentally bracketed ionization potential of GaAs lies above that of atomic gallium, implying that $D_0(\text{GaAs}) > D_0(\text{Ga}^+\text{–As})$. This in turn implies that the electron removed from GaAs when it is ionized is a bonding electron. Given that the molecule is primarily bound by σ electrons, the $\sigma^2\pi^2$, $^3\Sigma^-$ ground state of GaAs must be converted to a $\sigma\pi^2$, $^4\Sigma^-$ ground state of $GaAs^+$ upon ionization. This supposition is supported by theoretical calculations[23,25] and has been proved by ESR investigations of matrix isolated $GaAs^+$.[26]

It is also of interest to compare the chemical bonding in GaAs to that obtained in other III–V diatomics and group IV dimers, and to the bulk solid materials. This comparison is provided in Table IV. In the *p*-block elements, it is commonly recognized that $p\pi$ bonding becomes progressively less important as one moves down the periodic table toward heavier elements. Thus, for example, $p\pi$ bonding is favored over $p\sigma$ bonding in C_2,[7] leading to a π_u^4, $^1\Sigma_g^+$ ground state, but $p\sigma$ bonding is favored in Si_2,[8,9] leading to a $\sigma_g^2\pi_u^2$, $^3\Sigma_g^-$ ground state. This trend continues past Ge_2 (which is spectroscopically unknown in the gas phase), with both Sn_2[10] and Pb_2[11] characterized as O_g^+ ground states. In these latter systems strong off-diagonal spin–orbit interactions mix the $\sigma_g^2\pi_u^2$, $^3\Sigma_g^-$ (O_g^+) and $\sigma_g^2\pi_u^2$, $^1\Sigma_g^+$ (O_g^+) states, so that it is best to describe the states in case (c) nomenclature as simply O_g^+.

Among the mixed III–V diatomics, BN is the only system which has been spectroscopically characterized prior to this work. In diatomic BN, the strong propensity to form $p\pi$ bonds results in a ground state of $\sigma\pi^3$, $^3\Pi$,[13–15] rather than $\sigma^2\pi^2$, $^3\Sigma^-$ as found for GaAs. Again, the transition from favoring $p\pi$ bonding to favoring $p\sigma$ bonding occurs as one moves to heavier elements within a column of the periodic table. For BN, however, the propensity to form $p\pi$ bonds does not appear to be as strong as for C_2, as demonstrated by the $\sigma\pi^3$, $^3\Pi$ ground state of BN[13–15] as compared to the π_u^4, $^1\Sigma_g^+$ ground state of C_2.[7] The different ground state electronic configurations of BN and C_2 may be explained by considering the separated atom limits in each case. All three potential ground states of C_2 (π_u^4, $^1\Sigma_g^+$; $\sigma_g\pi_u^3$, $^3\Pi_u$; and $\sigma_g^2\pi_u^2$, and $^3\Sigma_g^-$) dissociate to ground state atoms ($^3P + {}^3P$). In this sense there is an even competition for the ground state, since none of these potential ground states require that an atom be promoted to an excited state. In BN, however, only the $\sigma\pi^3$, $^3\Pi$, and $\sigma^2\pi^2$, $^3\Sigma^-$ candidates for the ground state dissociate to ground state atoms. The π^4, $^1\Sigma^+$ analog of the ground state of C_2 is severely discriminated against, because it must dissociate to a $2s^22p$, $^2P^0$ ground state boron atom and an excited $2s^22p^3$, $^2D^0$ nitrogen atom. This separated atom limit lies 19 227 cm^{-1} above ground state atoms,[37] putting the π^4, $^1\Sigma^+$ state out of contention as the ground state of BN. On this uneven playing field, the emergence of $\sigma\pi^3$, $^3\Pi$ as the ground state of BN may be taken as evidence that $p\pi$ bonding is stronger than $p\sigma$ bonding in BN.

Interesting results are also obtained when one compares

TABLE IV. Comparison of gaseous diatomics and bulk semiconductors.

Group IV dimers		Group III–V diatomics	
C_2		BN	
$b\,^3\Sigma_g^-(\sigma_g^2\pi_u^2)\,T_e = 6434.2$ cm^{-1}	$r_e = 1.3692$ Å[a]		
$a\,^3\Pi_u(\sigma_g\pi_u^3)\,T_e = 716.2$ cm^{-1}	$r_e = 1.3119$ Å[a]		
$X\,^1\Sigma_g^+(\pi_u^4)$	$r_e = 1.2425$ Å[a]	$X\,^3\Pi(\sigma\pi^3)$	$r_e = 1.3096$ Å[c]
bulk (diamond)	$r = 1.5445$ Å[b]	bulk (zinc blende)	$r = 1.565$ Å[b]
Si_2		AlP	
$X\,^3\Sigma_g^-(\sigma_g^2\pi_u^2)$	$r_e = 2.246$ Å[d]	(Gas-phase spectroscopy is unknown)	
bulk (diamond)	$r = 2.352$ Å[b]	bulk (zinc blende)	$r = 2.360$ Å[e]
Ge_2		GaAs	
(Gas-phase spectroscopy is unknown)		$X\,^3\Sigma^-(\sigma^2\pi^2)$	$r_e = 2.53$ Å[f]
bulk (diamond)	$r = 2.450$ Å[b]	bulk (zinc blende)	$r = 2.446$ Å[e]
Sn_2		InSb	
$X\,O_g^+$	$r_e = 2.746$ Å[g]	(Gas-phase spectroscopy is unknown)	
bulk (diamond)	$r = 2.810$ Å[b]	bulk (zinc blende)	$r = 2.797$ Å[e]
Pb_2		TlBi	
$X\,O_g^+$	$r_e = 2.927$ Å[h]	(Gas-phase spectroscopy is unknown)	
bulk (fcc)	$r = 3.499$ Å[b]		

[a] Reference 7.
[b] Reference 39.
[c] Reference 15.
[d] References 8 and 9.
[e] Reference 40.
[f] This work.
[g] Reference 10.
[h] Reference 11.

the bond lengths of the ground state diatomic molecule to the nearest neighbor distances in the bulk materials (see Table IV). The group IV elements show an increase in interatomic distance upon formation of the bulk phase of 24.3%, 4.7%, 2.3%, and 19.5% for carbon, silicon, tin (diamond lattice structures), and lead (fcc), respectively. Likewise cubic BN (zinc blende structure) shows an increase in interatomic distance of 19.5% over gaseous, ground-state BN. Gallium arsenide, on the other hand, *contracts* by 3.32% upon condensation to bulk GaAs (zinc blende structure). The phenomenon of contraction upon condensation exhibited by GaAs is unique among the currently known group IV and group III–V diatomic molecules.

The first-row diatomics C_2 and BN display a large increase in bond length upon condensation into the diamond and zinc blende structures, because the multiple $p\pi$ bonds in these systems are converted to single σ bonds upon condensation. Such a large change in bond length is to be expected when such a gross change in bonding mechanism is encountered. In contrast, the chemical bonding in Si_2 and Sn_2 (and presumably, Ge_2) changes relatively little upon condensation into a diamond lattice, since the bonding in these diatomics is essentially just a single σ bond, with little additional stabilization from $p\pi$ bonding. In GaAs the change in interatomic spacing upon condensation is comparable to that found in Si_2 and Sn_2 (and presumably Ge_2), but is in the opposite direction. Very likely, the contraction which occurs upon condensation of GaAs is the result of an increased ionic contribution to the bonding in the solid as compared to the diatomic molecule. Such a possibility is absent in the homogeneous semiconductors, but is probably important in many of the III–V semiconductors. Accordingly, a contraction in interatomic distance upon condensation is likely to occur in AlP, AlAs, and GaP, just as has been observed in GaAs.

V. CONCLUSION

An optical spectrum of diatomic gallium arsenide has been observed using resonant two-photon ionization spectroscopy in a jet-cooled supersonic beam. To the best of our knowledge this represents the first spectrum of any kind to be obtained for diatomic GaAs. An analysis of the spectrum demonstrates that the ground state of GaAs is $X\,^3\Sigma^-$, deriving from the $\sigma^2\pi^2$ electronic configuration. The ground state is characterized by $\omega_e'' = 215\ \text{cm}^{-1}$, $\omega_e''x_e'' = 3\ \text{cm}^{-1}$, and $r_0'' = 2.53 \pm 0.02$ Å. The ground $X\,^3\Sigma^-$ state appears to have a large second-order spin–orbit interaction which places the $^3\Sigma_1^-$ component 43 cm^{-1} lower in energy than the $^3\Sigma_{0^+}^-$ component.

The observed excited state lies approximately 23 545 cm^{-1} above the ground state and has been shown to be a $^3\Pi_r$ state, which is split into $\Omega' = 2,1,0^+$, and 0^- components. The large splitting (23 cm^{-1}) between the 0^+ and 0^- components indicates that a nearby Σ state couples to one of these components, leading to a large Λ doubling which is nearly independent of J. Predissociation of the $^3\Pi_r$ levels is observed for $v' \geqslant 1$ for all Ω' values except for the $\Omega' = 0^+$ component. It is proposed that the upper states are predissociated by the $\sigma\sigma^*\pi^2$, $^5\Sigma^-$ state which correlates to separated atoms in their ground electronic states. This $^5\Sigma^-$ state possesses $\Omega = 2$, 1, and 0^- components and is coupled to the $\Omega' = 2$, 1, and 0^- levels of the $^3\Pi_r$ state by spin–orbit interaction, thereby inducing predissociation in these levels. Constants for the upper $^3\Pi_{0^+}$ state of $^{69}Ga^{75}As$ are: $\omega_e' = 152.13 \pm 0.70\ \text{cm}^{-1}$; $\omega_e'x_e' = 2.89 \pm 0.08\ \text{cm}^{-1}$; and $r_e' = 2.662 \pm 0.027$ Å.

The spectroscopic constants obtained in this study have been used to reevaluate the Knudsen effusion mass spectrometric measurement of the bond strength of GaAs, resulting in a conservative estimate of $D_0(\text{GaAs}) = 2.06 \pm 0.05$ eV. In addition, this study places the ionization potential of GaAs at $\text{IP}(\text{GaAs}) = 7.17 \pm 0.75$ eV.

Comparisons of diatomic GaAs to C_2, Si_2, Sn_2, Pb_2, and BN have also been made, supporting the notion that $p\pi$ bonding becomes less important as one moves to heavier p-block elements. Comparisons to the bulk solid materials show that GaAs is the only one of the abovementioned species for which the interatomic spacing decreases upon condensation to form the bulk material. It is suggested that the ionic contributions in bulk solid GaAs are more significant than in the diatomic, leading to stronger Coulomb attractions, which in turn cause the internuclear distance to decrease in the bulk solid. If this suggestion is correct, AlP, AlAs, and GaP should also exhibit a contraction as the bulk solid is built up from the diatomic molecules.

ACKNOWLEDGMENTS

The authors are grateful for the gift of gallium arsenide wafers from Standard Oil Research and Development of Ohio (BP America) and Morgan Semiconductor (Ethyl Corporation). We also thank Professor William H. Breckenridge for the use of the intracavity etalon and accessories employed in the high-resolution studies. We gratefully acknowledge research support from the National Science Foundation under Grant Nos. CHE-85-21050 and CHE-89-12673. Acknowledgment is also made to the donors of the Petroleum Research Fund, administered by the American Chemical Society, for partial support of this research.

[1] *Gallium Arsenide: Materials, Devices, and Circuits*, edited by M. J. Howes and D. V. Morgan (Wiley, New York, 1985).
[2] *Gallium Arsenide Technology*, edited by David K. Ferry (Sams, Indianapolis, 1985).
[3] N. W. Ashcroft and N. D. Mermin, *Solid State Physics* (Saunders College, Philadelphia, 1976), p. 566.
[4] C. H. Chen, C. A. Larsen, and G. B. Stringfellow, Appl. Phys. Lett. **50**, 218 (1987).
[5] C. A. Larsen, N. I. Buchan, and G. B. Stringfellow, Appl. Phys. Lett. **52**, 480 (1988).
[6] H. M. Manasevit, J. Cryst. Growth **55**, 1 (1981).
[7] K. P. Huber and G. Herzberg, *Molecular Spectra and Molecular Structure IV. Constants of Diatomic Molecules* (Van Nostrand Reinhold, New York, 1979).
[8] A. E. Douglas, Can. J. Phys. **33**, 801 (1955).

[9]R. D. Verma and P. A. Warsop, Can J. Phys. **41**, 152 (1963).
[10]V. E. Bondybey, M. Heaven, and T. A. Miller, J. Chem. Phys. **78**, 3593 (1983).
[11]M. C. Heaven, T. A. Miller, and V. E. Bondybey, J. Phys. Chem. **87**, 2072 (1983).
[12]P. F. Bernath, S. A. Rogers, L. C. O'Brien, C. R. Brazier, and A. D. McLean, Phys. Rev. Lett. **60**, 197 (1988).
[13]A. E. Douglas and G. Herzberg, Can. J. Res. A **18**, 179 (1940).
[14]B. A. Thrush, Nature **186**, 1044 (1960).
[15]H. Bredohl, I. Dubois, Y. Houbrechts, and P. Nzohabonayo, J. Mol. Spectrosc. **112**, 430 (1985).
[16]C. A. Stwarts, T. C. McGill, and W. A. Goddard III, Surf. Sci. **110**, 400 (1981).
[17]C. A. Stwarts, W. A. Goddard III, and T. C. McGill, J. Vac. Sci. Technol. **19**, 551 (1981).
[18]W. H. Lamfried and R. Strehlow, Phys. Status Solidi B **110**, K79 (1982).
[19]S. C. O'Brien, Y. Liu, Q. Zhang, J. R. Heath, F. K. Tittel, R. F. Curl, and R. E. Smalley, J. Chem. Phys. **84**, 4074 (1986).
[20]Y. Liu, Q. -L. Zhang, F. K. Tittel, R. F. Curl, and R. E. Smalley, J. Chem. Phys. **85**, 7434 (1986).
[21]W. D. Reents, Jr., J. Chem. Phys. **90**, 4258 (1989).
[22]K. Balasubramanian, Chem. Phys. Lett. **150**, 71 (1988).
[23]K. Balasubramanian, J. Chem. Phys. **86**, 3410 (1987).
[24]K. Balasubramanian, J. Chem. Phys. **87**, 3518 (1987).
[25]U. Meier, S. D. Peyerimhoff, P. J. Bruna, and F. Grein, J. Mol. Spectrosc. **134**, 259 (1989).
[26]L. B. Knight, Jr. and J. T. Petty, J. Chem. Phys. **88**, 481 (1987).
[27]Z. -W. Fu, G. W. Lemire, Y. Hamrick, S. Taylor, J. -C. Shui, and M. D. Morse, J. Chem. Phys. **88**, 3524 (1988).
[28]G. W. Lemire, Z. -W. Fu, Y. Hamrick, S. Taylor, and M. D. Morse, J. Phys. Chem. **93**, 2313 (1989).
[29]S. Taylor, G. W. Lemire, Y. Hamrick, Z. -W. Fu, and M. D. Morse, J. Chem. Phys. **89**, 5517 (1988).
[30]Z. -W. Fu and M. D. Morse, J. Chem. Phys. **90**, 3417 (1989).
[31]J. B. Hopkins, P. R. R. Langridge-Smith, M. D. Morse, and R. E. Smalley, J. Chem. Phys. **78**, 1627 (1983).
[32]G. Herzberg, *Molecular Spectra and Molecular Structure I. Spectra of Diatomic Molecules*, 2nd ed. (Van Nostrand Reinhold, New York, 1950).
[33]S. Gerstenkorn and P. Luc, *Atlas du Spectre d'Absorption de la Molecule d'Iode* (CNRS, Paris, France, 1978).
[34]S. Gerstenkorn and P. Luc, Rev. Phys. Appl. **14**, 791 (1979).
[35]P. R. R. Langridge-Smith, M. D. Morse, G. P. Hansen, R. E. Smalley, and A. J. Merer, J. Chem. Phys. **80**, 593 (1984).
[36]H. Lefebvre-Brion and R. W. Field, *Perturbations in the Spectra of Diatomic Molecules* (Academic, Orlando, 1986).
[37]C. E. Moore, Natl. Bur. Stand. Circ. No. 467 (1971), Vol. II.
[38]G. DeMaria, L. Malaspina, and V. Piacente, J. Chem. Phys. **52**, 1019 (1970).
[39]N. L. Greenwood and A. Earnshaw, *Chemistry of the Elements* (Pergamon, Oxford, 1984).
[40]C. Kittel, *Introduction to Solid State Physics*, 6th ed. (Wiley, New York, 1986), p. 20.
[41]K. Balasubramanian, J. Mol. Spectrosc. (in press).